Mitigating Degree Bias Adaptively with Hard-to-Learn Nodes in Graph Contrastive Learning

Jingyu Hu
University of Bristol
ym21669@bristol.ac.uk

Hongbo Bo
University of Bristol
hongbo.bo@bristol.ac.uk

Jun Hong
University of the West of England
jun.hong@uwe.ac.uk

Xiaowei Liu
University of Bristol
xiaowei.liu@bristol.ac.uk

Weiru Liu
University of Bristol
weiru.liu@bristol.ac.uk

Abstract

Graph Neural Networks (GNNs) often suffer from degree bias in node classification tasks, where prediction performance varies across nodes with different degrees. Several approaches, which adopt Graph Contrastive Learning (GCL), have been proposed to mitigate this bias. However, the limited number of positive pairs and the equal weighting of all positives and negatives in GCL still lead to low-degree nodes acquiring insufficient and noisy information. This paper proposes the Hardness Adaptive Reweighted (HAR) contrastive loss to mitigate degree bias. It adds more positive pairs by leveraging node labels and adaptively weights positive and negative pairs based on their learning hardness. In addition, we develop an experimental framework named SHARP to extend HAR to a broader range of scenarios. Both our theoretical analysis and experiments validate the effectiveness of SHARP. The experimental results across four datasets show that SHARP achieves better performance against baselines at both global and degree levels. **Keywords:** Degree Bias, Graph Contrastive Learning, Adaptive Learning, Node Classification

1 Introduction

One common approach to graph representation learning is to use a Graph Neural Network (GNN) like a Graph Convolutional Network (GCN) (Kipf and Welling, 2016) to learn graph embeddings. These learned embeddings have proven effective in many downstream tasks. However, most of these studies have focused mainly on global performance, while their subgroup-level performance has often been overlooked. Though their global performance is good, recent studies (Tang et al., 2020; Liu et al., 2023) have shown that the predictions of GNNs can exhibit structural unfairness. In node classification tasks, GNNs tend to perform better on high-degree nodes than low-degree ones (Liu et al., 2023; Wang et al., 2022). This is also known as degree bias: the performance disparity across nodes with different degrees.

One of the most common observations on the origin of degree bias is that the neighborhoods of low-degree nodes provide insufficient and noisy information for generating their effective representations (Subramonian et al., 2024; Tang et al., 2020). GNNs learn node representations by aggregating feature information from neighbourhoods. High-degree nodes, with more neighbors, can collect a richer set of features than low-degree nodes. Furthermore, as the few neighbors of the low-degree node may come from different classes, the aggregated noisy information can even confuse the GNNs in classification tasks. Figure 1 (Left) shows a degree bias example of using a GNN to classify occupations, where GNNs can achieve worse performance for low-degree (painter, conductor) nodes compared to high-degree nodes (music producer). For instance, when GNNs classify the conductor node, they will aggregate features from its neighbors (two producer nodes); this noisy information can mislead the model into classifying it as a producer rather than a conductor.

Recent studies (Wang et al., 2022; Kose and Shen, 2022; Ling et al., 2023) have found that applying Graph Contrastive Learning (GCL) can help achieve fair representation learning. GCL (Zhu et al., 2020, 2021) combines GNNs with contrastive learning (Chen et al., 2020; He et al., 2020). The typical GCL framework first generates two augmented views based on the transformation to the features and edges of the node, then defines a contrastive loss function to learn node representations from the generated graph views. GCL can mitigate degree bias to some extent by reducing the model's reliance on neighbourhoods by introducing augmented views. The contrastive loss in GCL pulls positives closer while pushing negatives apart. For each node, the commonly adopted contrastive loss considers only the two augmented views as

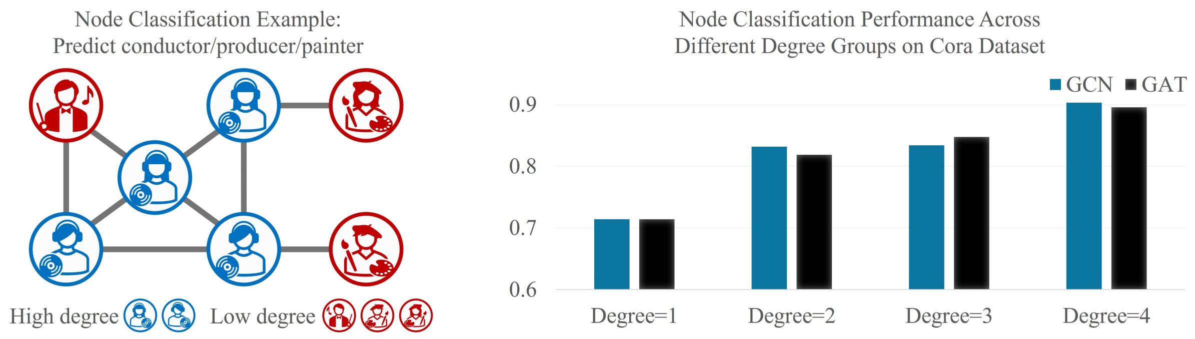

Figure 1: (Left.) The degree bias example in node classification: GNNs can perform worse on low-degree nodes (e.g., painter, conductor) than on high-degree nodes (e.g., producer) due to insufficient or noisy information from neighboring nodes for low-degree nodes. (Right.) Empirical results of degree bias. The different prediction performances across different degree groups on Cora: Low-degree nodes tend to have lower utility performance compared to high-degree nodes.

positives, and all other nodes as negatives.

This assumption often leads to insufficient positive pair sampling for low-degree nodes which disadvantages them. One positive pair is insufficient to adequately support low-degree nodes, and degree bias still persists. Supervised contrastive learning loss (SCL) (Khosla et al., 2020) provides one solution by introducing more positive pairs for low-degree nodes. SCL treats all nodes of the same class as positives and all the other nodes as negatives, and assigns equal weights to every node. However, as the example shown in Figure 1, different nodes have different levels of learning hardness: Some are more informative and help form a clearer embedding space, whereas the others can contain noisier information to adversarially affect the latent space structure learning. Assigning equal weights to noisy nodes may prevent the model from capturing more important information.

In this paper, we propose a new contrastive loss that (1) includes more positives and (2) assigns different weights to positives and negatives to focus more on those with important information and less on the others with noisy information, thereby mitigating degree bias. We first apply SCL to ensure sufficient positives. Then, we design *learning hardness* to quantify how hard each node is to learn. For each node, both its augmented nodes and nodes from different classes with which the node shares high similarity are treated as hard-to-learn nodes. We propose Hardness Adaptive Reweighted (HAR) contrastive loss that adaptively assigns higher weights to hard-to-learn nodes and lower weights to easier ones, ensuring the model focuses on the hard-to-learn cases. Providing additional and more accurate information for low-degree nodes, which originally has insufficient information, helps accelerate their representation learning and reduce degree bias.

In addition, we extend our HAR loss to the semi-supervised GCL scenario to validate its adaptivity in real-world applications where not all samples are labelled. Specifically, we separate the training data into two subsets—the labelled and unlabelled parts—to simulate the scenario where part of the training data is unlabelled. Our proposed Semi-supervised Hardness Adaptive Reweighted with Pseudo-labels (SHARP) consists of two steps. First, the model is pre-trained using the labelled training data. Second, the pre-trained model generates pseudo-labels for the unlabelled training data. We then use the pseudo-labelled training data to further fine-tune the model. Both pre-training and fine-tuning follow the GCL workflow. Overall, the main contributions of the paper are as follows:

- **Hardness Adaptive Reweighted (HAR)** contrastive loss is proposed to address the degree bias. It provides more accurate positives and negatives for low-degree nodes, and assigns them adaptive weights. It enables the model to focus more on important information and less on noisy information. Our results show that low-degree nodes benefit more from adaptive weighting.

- **Empirical and Theoretical Analysis** We extend the application of HAR to the semi-supervised setting and propose the SHARP framework to validate HAR's adaptivity in broader scenarios. Our theoretical analysis also proves that (1) our proposed HAR loss is bounded and (2) even under the worst-case hyperparameter settings, the misclassification risk of SHARP also remains bounded.

- **Extensive Experiments** are performed across four datasets using two different GNN encoders, comparing our approach with four baselines. The results show SHARP's effective degree bias mitigation without adversally affecting the overall performance. Globally, our SHARP can achieve comparative prediction performance with fewer labelled samples (even with 50% fewer). Visualization of the latent feature space also validates that SHARP can produce clearer class boundaries. At the node degree level, SHARP shows particular enhancement in low-degree groups.

2 Related Work

2.1 Graph Representation Learning

Graph representation learning embeds graph-structured data into a feature space. The learned graph representations are generally integrated with task-specific neural networks to perform downstream tasks at various levels: graph-level, link-level, or node-level. This paper focuses on node-level tasks, which aim to predict the label of each node in a graph. GNNs and GCL are two common ways of generating embeddings for node classification tasks.

Graph Neural Networks (GNNs) are proposed to extend neural networks to process graph-structured data which has nodes features and connections between nodes. The core idea of GNNs is message passing between nodes, updating feature values by considering connected nodes layer by layer. Graph layers (GLs) define how nodes send, receive, and update messages. Convolution-based (e.g., GCN (Kipf and Welling, 2016)), attention-based (e.g., GAT (Veličković et al., 2017)), and aggregation-based (e.g., GraphSAGE (Hamilton et al., 2017)) are three common types of graph layers (Bronstein et al., 2021).

Graph Contrastive Learning (GCL) combines GNNs with Contrastive Learning (CL) which enhances the robustness of learned representations. CL is a learning scheme that focuses on pulling similar/positive samples closer while pushing dissimilar/negative samples away using a contrastive loss. Despite the abundance of contrastive loss variations (Chen et al., 2020; Assran et al., 2020; Khosla et al., 2020), most GCL methods still use the common contrastive loss: it treats two augmented node originated from the same node as the positive pair, while treating all others as equally important negatives. This can make it hard to handle degree bias as we will discuss in detail below.

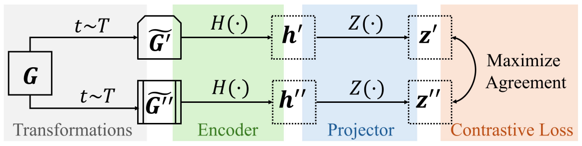

Figure 2: The Workflow of Contrastive Learning

2.2 Degree Bias in Node Classification

Based on graph connectivity, nodes can be split into low-degree and high-degree groups. (Zhao and Jia, 2024; Subramonian et al., 2024) show that GNNs tend to have higher utility for high-degree nodes than low-degree nodes. This difference in prediction performance across nodes with different degrees is referred to as degree bias. (Subramonian et al., 2024) provides a detailed theoretical analysis and summarizes common hypotheses of degree bias origins, which the most common hypotheses is that neighborhoods of low-degree nodes contain insufficient and noisy information (Feng et al., 2021; Xiao et al., 2021).

Bias Mitigation Methods Many GNN-based degree bias mitigation methods (Yun et al., 2022; Kang and Tong, 2021; Liang et al., 2023) have been proposed. For example, (Liu et al., 2021) introduced the concept of transferable neighborhood translation, which can transfer information from high-degree nodes to low-degree nodes to enhance their representations. (Han et al., 2024) proposes a hop-aware attentive information aggregation scheme to expand the neighborhood for marginal nodes, thereby achieving structural fairness.

Recent work (Wang et al., 2022) found that GCL exhibits better structural fairness and less degree bias, compared with pure GNNs. GRACE (Zhu et al., 2020) applies GCL to node classification by generating contrastive views through the random masking of nodes and edges. To further mitigate degree bias, many GCL-based mitigation methods have been proposed. GRADE (Wang et al., 2022) proposed a pre-defined graph augmentation pattern. Specifically, it follows the process of GRACE with a modified random edge-dropping scheme by deliberately dropping edges for high-degree nodes while adding edges for low-degree nodes. (Zhang et al., 2023) applies random graph coarsening to data augmentation in GCL and mitigates degree bias by contrasting the coarsened graph with the original graph. (Kose and Shen, 2022) introduces adaptive graph augmentation to make GCL fairness-aware. Furthermore, (Zhao and Jia, 2024) performs GCL on heterogeneous graphs to mitigate degree bias.

These GCL mitigation methods generally tackle degree bias by introducing optimized data augmentation in the pre-processing stage, while still using the common contrastive loss. However, the common contrastive loss has two underlying limitations: (1) It considers only one positive pair per node. For low-degree nodes with few connections, this restricts their information gathering. (2) It assumes all positives and negatives contribute equally to the loss function. However, some of them can contain more important information and are harder to learn in practice.

To address these issues and mitigate degree bias, we propose a new contrastive loss that (1) is specifically designed to identify positive and negative pairs based on label information, allowing low-degree nodes to learn more information, and (2) assigns adaptive weights based on learning hardness to provide tailored information, enabling low-degree nodes to receive less noise and more focused learning.

3 Methodology

We begin with a brief introduction to the basics of graph contrastive learning. This is followed by a detailed description of our proposed Hardness Adaptive Reweighted (HAR) loss, which helps mitigate degree bias. Last, we describe an experimental pipeline named SHARP that extends HAR loss across broader scenarios for enhanced robustness.

3.1 Preliminary

The graph data is denoted as $G = (V, E)$, where V is a set of N nodes, and E is the set of edges. In the node classification task, each node $v \in V$ has an associated label y and a M-length feature vector $x \in X$. Each edge $e \in E$ refers to the nodes connection pair, denoted as $e = (v_i, v_j)$, where $i, j \in \{1, 2, ..., N\}$. We define $X_{N \times M}$ as the feature matrix of V, $Y_{N \times 1}$ as the labels set, and $A_{N \times N}$ as the adjacency matrix where $A_{ij} = 1$ if $(v_i, v_j) \in E$ or $i = j$, and 0 otherwise. The degree of v is the number of edges connected to it.

As shown in Figure 2, graph contrastive learning methods generally follow a similar workflow (Chen et al., 2020; Zhu et al., 2020; Wang et al., 2022). First, two augmented views, $\tilde{G}'$ and $\tilde{G}''$, are generated from the given graph G using transformation techniques like perturbation, removal, noise addition, etc. We follow the transformation practice in (Zhu et al., 2020; Srivastava et al., 2014) to perform random masking on both edges and node features to form $\tilde{G}'$ and $\tilde{G}''$.

- **Masking Edges (ME)** Some edges are randomly removed from the original graph with an edge dropping rate P_e. We generate a random masking matrix $\tilde{R}_{N \times N} \in \{0, 1\}$, where each entry is sampled from a Bernoulli distribution $\tilde{R}_{ij} \sim \mathcal{B}(1 - p_e)$ where $\tilde{R}_{ij} = 1$ if $A_{ij} = 1$ in the original graph, and $\tilde{R}_{ij} = 0$ otherwise. The new adjacency matrix $\tilde{A}$ is obtained by performing the Hadamard product of A and $\tilde{R}$, denoted as $\tilde{A} = A \circ \tilde{R}$.

- **Masking Features (MF)** Similarly, features are randomly masked with a feature dropping rate p_f. Each dimension of the features masking vector $\tilde{\mathbf{r}} \in \{0, 1\}^M$ is independently sampled following a Bernoulli distribution with probability $(1 - p_f)$. Each node features $\tilde{x_i}$ are calculated by Hadamard product between $\tilde{\mathbf{r}}$ and each node feature vector x_i where $i \in \{1, 2, \ldots N\}$. Then the masked feature matrix is obtained by concatenating the masked feature vectors, denoted as $\tilde{X} = [x_1 \circ \tilde{\mathbf{r}}; x_2 \circ \tilde{\mathbf{r}}; \cdots; x_N \circ \tilde{\mathbf{r}}]^\top$.

Then, an encoder $H(\cdot)$ is used to produce data embeddings h' and h'' for the augmented views. A projection head $Z(\cdot)$ further maps embeddings h' and h'' into the space z' and z''. Here we set GNNs as the encoder $H(\cdot)$ and MLP as the projector $Z(\cdot)$. Last, the contrastive loss is calculated from z' and z''. In each training epoch, parameters are updated to minimize contrastive loss.

3.2 The Proposed Hardness Adaptive Reweighted Contrastive Loss

Figure 3 shows the workflow of our proposed Hardness Adaptive Reweighted (HAR) contrastive loss. Our HAR adaptively assigns weights to each node's positives and negatives based on nodes learning hardness. This novel weighting strategy

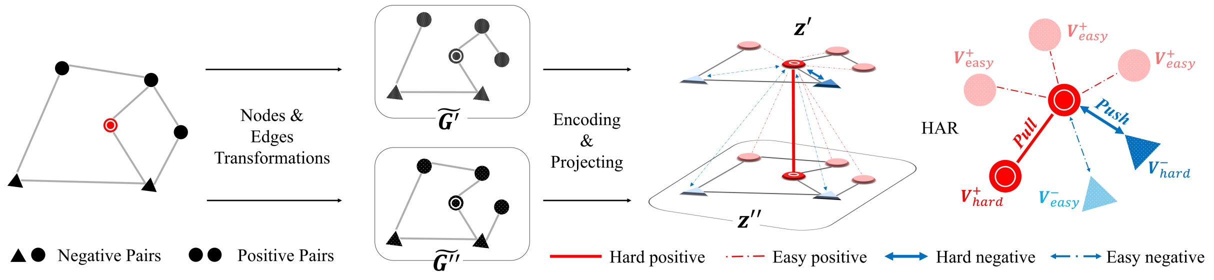

Figure 3: The Illustration of Graph Contrastive Learning with Our Proposed HAR Loss

Table 1: Hard/Easy and Positive/Negative Node Definitions for Each Given Node v_i.

Categories	**Descriptions**
Hard Negative Nodes $\mathbf{v}^-_{hard}$	Nodes with Different Labels $(y_i \neq y_j)$ but High $f_\tau(z_i, z_j)$
Easy Negative Nodes $\mathbf{v}^-_{easy}$	Nodes with Different Labels $(y_i \neq y_j)$ and Low $f_\tau(z_i, z_j)$
Hard Positive Nodes $\mathbf{v}^+_{hard}$	Nodes with Same Label $(y_i = y_j)$ and Same Origin
Easy Positive Nodes $\mathbf{v}^+_{easy}$	Nodes with Same Label $(y_i = y_j)$ but Different Origins

can effectively address degree bias issue. We first present our definitions of positives, negatives, and learning hardness, then describe HAR's adaptive weighting mechanism.

For a given node v_i, its relationship with other nodes v_j $(j \in \{1, 2, ..., N\})$ can be categoriesed into hard negatives $\mathbf{v}^-_{hard}$, easy negatives $\mathbf{v}^-_{easy}$, hard positives $\mathbf{v}^+_{hard}$, and easy positives $\mathbf{v}^+_{easy}$, as defines in Table 1. Nodes are treated as positives $\mathbf{v}^+$ if they have the same label, and as negatives $\mathbf{v}^-$ otherwise. We define the *learning hardness* of $\mathbf{v}^+$ based on augmentation origin[1], while that of $\mathbf{v}^-$ on similarity between their representations $f_\tau(z_i, z_j)$ as defined in Equation (1). Intuitively, hard-to-learn nodes include nodes with the same origin (hard positives) and those highly similar but in different classes (hard negatives).

$$f_\tau(z_i, z_j) = \exp(\text{sim}(z_i, z_j)/\tau), \tag{1}$$

$$\text{sim}(z_i, z_j) = \frac{z_i \cdot z_j}{\|z_i\| \|z_j\|}. \tag{2}$$

Based on the definitions, we can form Equation (3) to obtain the overall positive mask matrix Mask$^+$ and negative mask matrix Mask$^-$ by identifying the positive and negative samples for each node. $\mathbb{I}$ is an indicator function, where $\mathbb{I}_{(y_i=y_j)}$ takes the value 1 iff y_i and y_j are the same, and 0 otherwise. Similar notation applies to $\mathbb{I}_{(y_i \neq y_j)}$.

$$\text{Mask}^+ = [\mathbb{I}_{(y_i=y_j)}]_{N\times N}, \text{Mask}^- = [\mathbb{I}_{(y_i\neq y_j)}]_{N\times N} \tag{3}$$

Equation (4) defines the similarity matrix S to incorporate association information between nodes from two sources: **intra-view** associations (within the embedding representation from the same view, such as within z' or z'') and **inter-view** associations (across different views, like between z' and z'').

$$S = [s_{i,j}]_{N\times N}, s_{i,j} = \underbrace{f_\tau(z'_i, z'_j)}_{\text{inter-view}} + \underbrace{f_\tau(z'_i, z''_j)}_{\text{intra-view}} \tag{4}$$

The corresponding similarity matrices for positive samples S^+ and negative samples S^- can be formed by Equation (5), where $\circ$ denotes the Hadamard product. $S^+_{i,j}$ and $S^-_{i,j}$ means the values of S^+ and S^- at (i, j).

$$S^+ = S \circ \text{Mask}^+, S^- = S \circ \text{Mask}^-. \tag{5}$$

For positive pairs, we aim to encourage the model to focus more on learning the representation of the sample itself $\mathbf{v}^+_{hard}$, while also considering information from other positive samples $\mathbf{v}^+_{easy}$. Therefore, we first scale S^+ to assign adaptive weights to all positive samples, then add extra weights to $\mathbf{v}^+_{hard}$ via a $N \times N$ identity matrix $\mathbf{I}_N$. The reweighted positives are defined by Equation (8).

[1]For any augmented node $v'_a \in \tilde{G}'$, its augmentation origin is defined as the corresponding original node $v_a \in G$. Two augmented nodes (eg. $v'_a \in \tilde{G}', v''_b \in \tilde{G}''$) have the same origin if their augmentation origins are the same $(v_a = v_b)$, and have different origins otherwise $(v_a \neq v_b)$.

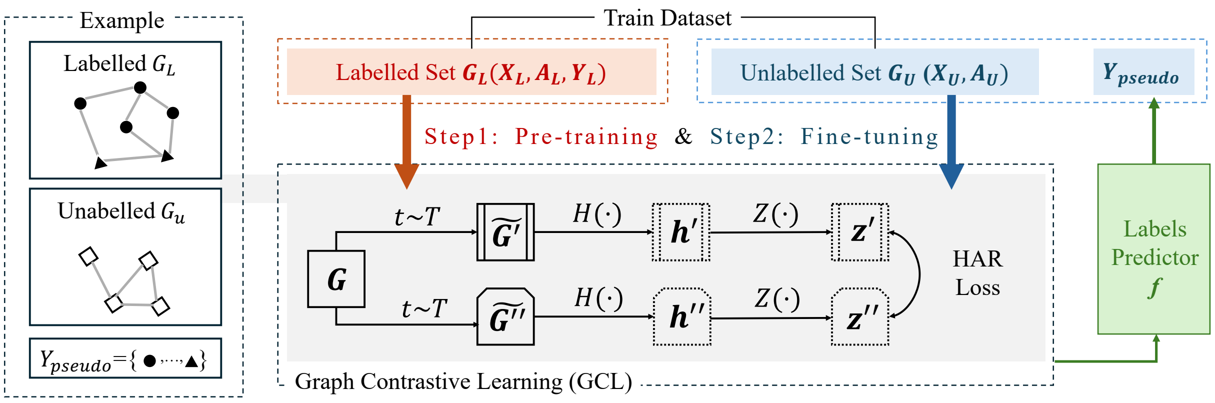

Figure 4: The Two-Step SHARP with HAR Loss on Node Classification Tasks

$$W^+ = \alpha \cdot \bar{S}^+ + \mathbf{I}_N, \tag{6}$$

$$\bar{S}^+ = [\bar{s}_{ij}]_{N\times N}, \bar{s}_{ij} = \frac{\max(S^+) - S^+_{ij}}{\max(S^+) - \min(S^+)}. \tag{7}$$

$$\mathrm{POS}_i = \sum\nolimits_{j=1}^{N} (W^+_{ij} \cdot S^+_{ij}) \tag{8}$$

For negative samples, we refer to CL in debiasing (Chuang et al., 2020) and reweighting (Kalantidis et al., 2020) strategies which assigns higher weights to $\mathbf{v}^-_{hard}$ and lower weights to $\mathbf{v}^-_{easy}$.

The reweighted negatives are defined by Equation (9), where β is the scaling term; τ^+ is a class probability and is calculated as the reciprocal of the number of classes; and Q_i represents the ratio between positive and negative sample counts for node v_i, defined as $\frac{CNT_i(\mathrm{Mask}^-)}{CNT_i(\mathrm{Mask}^+)}$.

$$W^- = [w^-_{ij}]_{N\times N}, w^-_{i,j} = \frac{\beta \cdot S^-_{ij}}{\frac{1}{N}\sum_{j=1}^{N} S^-_{ij}}.$$

$$\mathrm{NEG}_i = \max\left(\frac{\sum_{j=1}^{N}(-Q_i \cdot \tau^+ \cdot S^+ + W^- \cdot S^-)}{1-\tau^+}, e^{-\frac{1}{\tau}}\right) \tag{9}$$

After gaining the new weighted similarities for both positives and negatives, the loss for node v_i is defined as Equation (10).

$$\ell_i(z', z'') = -\log \frac{\mathrm{POS}_i}{\mathrm{POS}_i + \mathrm{NEG}_i} \tag{10}$$

Given the symmetry between the two contrasting perspectives, the overall HAR contrastive loss for the input graph data G is designed as follows.

$$HAR = \frac{1}{2N}\sum_{i=1}^{N}\left[\ell_i(z', z'') + \ell_i(z'', z')\right] \tag{11}$$

Theoretical Analysis We present the theoretical analysis of two hyper-parameters associated with the distributions of positive and negative samples based on previous analyses (Robinson et al., 2021). Our findings show that even under worst-case hyperparameter settings, the misclassification risk of SHARP remains bounded. Specifically, SHARP degenerates to the case in (Robinson et al., 2021) when $\alpha = 0$, and for a fixed β, we observe that the upper bound of the loss function is reached due to the monotonicity property of the logarithm function. Furthermore, HAR loss does not exceed that of the aforementioned fully unsupervised objective function. The details are provided in Appendix C.

3.3 The Extension: Two-step SHARP Framework

To validate the effectiveness of our HAR loss in real-world cases where labels may not always be available, we design a two-step training framework that extends the application of our HAR loss to the semi-supervised scenario. We call the proposed framework as SHARP (Semi-supervised Hardness Adaptive Reweighted with Pseudo-labels) as shown in Figure 4.

Specifically, we split training data into two sets $G_{\text{train}} = G^L_{\text{train}} \cup G^U_{\text{train}}$ where labelled train set is denoted as $G^L_{\text{train}} = \{X_L, A_L, Y_L\}$ and unlabelled data is denoted as $G^U_{\text{train}} = \{X_U, A_U, \emptyset\}$. The overall training process consists of two steps: First, the GCL is applied to the labelled data G^L_{train} to generate a pre-trained model. Second, the pre-trained model is used to generate the pseudo-labels for G^U_{train}. The new $G^U_{\text{train}} = \{X_U, A_U, Y_{pseudo}\}$ is then fed into the GCL for further fine-tuning the pre-trained model. Both steps are in the same GCL workflow with HAR loss, using their respective datasets.

4 Experiments and Results

This section first describes the experimental setup, followed by a global performance comparison and a detailed analysis across degree groups. We last present our parameter sensitivity analysis and dimension reduction visualization to confirm the effectiveness of our method, supporting the validity of the results.

4.1 Experiment Settings

Datasets The experiments are run on four datasets with node classification tasks: Cora (McCallum et al., 2000), CiteSeer (Giles et al., 1998), PubMed (Sen et al., 2008), and Wiki-CS (Mernyei and Cangea, 2020). The first three datasets are paper citation networks on different domains, Wiki-CS contains Wikipedia articles in computer science topics, and all aiming to predict specific topic of each node.

Table 2: Dataset Statistics

Dataset	Type	Nodes	Edges	Classes	Features
Cora	Citation	2,708	5,429	7	1,433
Citeseer	Citation	3,327	4,732	6	3,703
Pubmed	Citation	19,717	44,338	3	500
Wiki-CS	Wikipedia	11,701	216,123	10	300

Graph Contrastive Learning Settings Our graph learning processing is based on PyG package (Fey and Lenssen, 2019). We run experiments on both two-layer GCN and GAT as the encoder, the projector is set to be a two-layer Multilayer Perceptron (MLP). The contrastive loss is implemented as the proposed HAR. The parameters setting like edge dropping rate p_e, feature dropping rate p_f, temperature τ, etc., are listed in the Appendix B.

Two-step Learning Settings We follow (Sen et al., 2008; Kipf and Welling, 2016) to split the data into train G_{train}, validation G_{val} and test G_{test} datasets. Then, G_{train} is splitted into two parts: a fraction $r \in [0, 1)$ forms the unlabelled sub-training set $G^{\text{U}}_{\text{train}}$, while the remainder forms the labelled sub-training set $G^{\text{L}}_{\text{train}}$. First, the model is pre-trained with $G^{\text{L}}_{\text{train}}$ for *epoch* rounds. In the following model fine-tuning on the $G^{\text{U}}_{\text{train}}$, we validate the prediction performance on the validation set G_{val} for each round and record the best history result. When the best result is not updated for K rounds, we stop the training and save the encoder. The model evaluation is based on embeddings of G_{test} generated from this saved encoder.

Baselines One GNN-based and three GCL-based methods are set as baselines. All GCL-based methods follow the same GCL workflow and with different contrastive losses (GRACE (Zhu et al., 2020), SCL (Khosla et al., 2020), Debias (Chuang et al., 2020)). The final embeddings are then fed into a logistic regression classifier for performance evaluation. To ensure results comparability, all baselines follow the same two-step semi-supervised learning: pre-training their respective initial performance on the $G^{\text{L}}_{\text{train}}$, and fine-tuning on the $G^{\text{U}}_{\text{train}}$.

Evaluation All evaluations are under the test set G_{test} using F1-score as the metric. Each model is run 10 times, and we report the mean scores. F1-score is set as our evaluation metric as it is derived from Precision and Recall—which in turn are calculated based on the values of True Positives (TP), False Positives (FP), False Negatives (FN), and True Negatives (TN) in the confusion matrix—providing a more balanced measure of performance. We perform both global and degree-level evaluations: (1) The global evaluation computes performance across the entire test set. (2) For degree-level evaluation, we group test data by node degrees and compute F1-score within each degree group. The degree bias is assessed by comparing performance disparities among degree groups.

4.2 Result Discussions

The results show SHARP's performance at the global and degree levels. The robustness of SHARP is examined through experiments with different hyperparameter combinations and latent embedding visualizations.

4.2.1 Global Level Performance

Table 3 illustrates the global F1-score performance of five models across four datasets. Compared to GRACE, which only treats one single positive pair, SCL, Debias, and SHARP all utilize labels to customize positives and negatives for each node, and their overall performance is better than GRACE. Our SHARP outperforms the baseline in 14 out of 16 tests and shows most significant improvement on the Cora dataset, with a 3.6% increase in performance under the GCN layer ($r = 0$) and a 4.2% increase under the GAT layer ($r = 0$) setting. SHARP performs slightly lower than SCL and Debias on the PubMed dataset ($r = 0.3$). This

Table 3: Prediction Performance Comparison across Different Models on F1-Score

GCN as Graph Layers					GAT as Graph Layers				
$r = 0$	Cora	CiteSeer	PubMed	Wiki-CS	$r = 0$	Cora	CiteSeer	PubMed	Wiki-CS
GCN	0.8340	0.7140	0.8630	0.8116	GAT	0.8345	0.7230	0.8690	0.8214
GRACE	0.7992	0.6914	0.8392	0.7487	GRACE	0.7928	0.6790	0.8388	0.7568
SCL	0.8176	0.7202	0.8926	0.8027	SCL	0.8415	0.7218	0.8814	0.8070
Debias	0.8152	0.7226	0.8906	0.8062	Debias	0.8465	0.7196	0.8837	0.8095
SHARP(Ours)	**0.8700**	**0.7252**	**0.8942**	**0.8193**	SHARP(Ours)	**0.8770**	**0.726**	**0.8931**	**0.8235**
$r = 0.3$	Cora	CiteSeer	PubMed	Wiki-CS	$r = 0.3$	Cora	CiteSeer	PubMed	Wiki-CS
GCN	0.8170	0.7120	0.8740	0.8078	GAT	0.8260	0.7090	0.8640	0.7975
GRACE	0.7839	0.6938	0.8354	0.7499	GRACE	0.7948	0.6976	0.8410	0.7513
SCL	0.7804	0.7117	0.8860	0.8002	SCL	0.8318	0.7188	**0.8830**	0.8017
Debias	0.7846	0.7100	**0.8872**	0.8011	Debias	0.8254	0.7224	0.8814	0.8007
SHARP(Ours)	**0.8586**	**0.7212**	0.8856	**0.8150**	SHARP(Ours)	**0.8667**	**0.7268**	0.8809	**0.8191**

can be due to our current simple semi-supervised scheme for all baselines, which applies a fixed-step early stopping strategy during the second-step fine-tuning process, potentially introducing fluctuations to the results. We focus on how GCL settings benefits graph structural fairness in this paper, and leave the discussion of different fine-tuning strategies in semi-supervised learning for future work.

4.2.2 Degree Level Performance

Besides overall performance, we also analyze degree bias by comparing performance across degree groups. Small sample sizes in some very high-degree groups can reduce performance confidence. Thereby we focus on nodes with degrees 0 to 7 to ensure sufficient samples within degree groups. Figure 6(a) illustrates degree-level performance on the Cora dataset ($r = 0.3$). Among all methods, SHARP shows the most significant improvement for low-degree nodes, achieving over 10% increase for the node group (degree=1) compared to the GAT baseline. Comparing growth rates across subgroups, SHARP enhancement for low-degree nodes is higher than high-degree group. Similar trends are also in PubMed datasets (Table 4). Despite limited global improvement discussed above, subgroup analysis shows SHARP focuses on boosting scores for low-degree nodes, narrowing the performance gap with high-degree nodes. Therefore, we conclude our method shows a targeted improvement, particularly benefiting low-degree nodes across datasets, addressing the uneven performance on different node degree groups.

To further investigate why our method can reduce degree bias, we further analyze the degree distributions of hard-to-learn nodes. For each node, the top hard-to-learn nodes (those assigned higher weights) are identified. Then, the degrees of these selected nodes are recorded and their degree distributions are visualized using Kernel Density Estimation[2].

Figure 5 displays degree distribution comparisons of Top-5 hard negatives across different training epochs. The gray area represents the original distribution without adaptive weights, serving as our ablation study. The proportion of low-degree nodes in the hard-to-learn nodes distribution is higher than the base distribution. Assigning higher weights to hard-to-lean nodes puts more focus on low-degree nodes during training and helps mitigate degree bias. Traditional equal weighting fails to explore the full potential of low-degree nodes.

4.2.3 Parameters Sensitivity Analysis

To assess parameter sensitivity, additional experiments are performed with different proportions of unlabelled data $r \in [0, 1)$, and the hyperparameters $\alpha \in (0, 1]$ and $\beta \in (0, 1]$. Figure 6(b)(c) shows the comparison results on the Cora dataset. The results are generally robust to the scaling parameters α and β, with performance varying by less

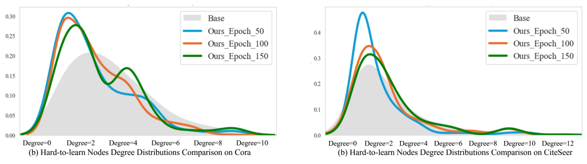

Figure 5: The Node Degree Distributions of Top-5 Hard Negatives (GAT layers, $r = 0$)

[2]The KDE plot smooths data with a Gaussian kernel for a continuous density estimate.

Table 4: Degree-level Prediction Performance Comparison on PubMed Dataset (GAT as the graph layers, $r = 0$, Δ indicates changes compared with the GAT baseline)

Degree	Size	GAT	GRACE	Δ	SCL	Δ	Debias	Δ	SHARP(Ours)	Δ
1	483	0.8364	0.8023	-3.41%	0.8553	1.89%	0.8553	1.89%	0.8706	**3.42%**
2	153	0.8824	0.8471	-3.53%	0.9000	1.76%	0.9007	1.83%	0.9190	**3.66%**
3	79	0.9367	0.9051	-3.16%	0.9519	1.52%	0.9481	1.14%	0.9519	**1.52%**
4	40	0.9250	0.8600	-6.50%	0.9500	2.50%	0.9500	2.50%	0.9750	**5.00%**
5	35	0.8857	0.8600	-2.57%	0.9143	**2.86%**	0.9229	**3.72%**	0.8971	1.14%
6	28	0.8571	0.8750	1.79%	0.8929	**3.58%**	0.8929	**3.58%**	0.8929	**3.58%**
7	14	0.9286	0.9357	0.71%	1.0000	**7.14%**	0.9714	4.28%	0.9286	0.00%

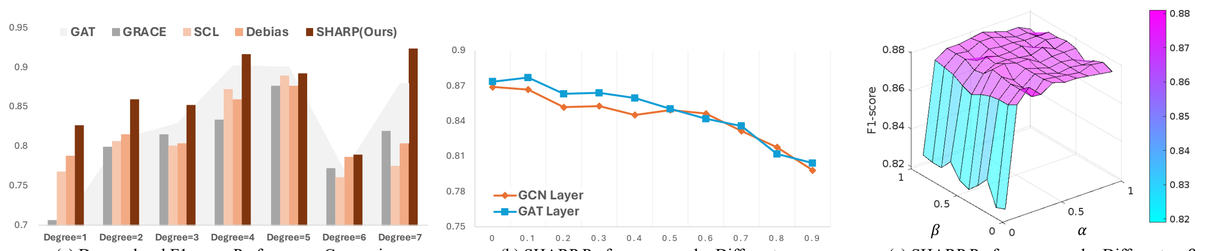

(a) Degree-level F1-score Performance Comparison (b) SHARP Performance under Different r (c) SHARP Performance under Different α, β

Figure 6: (a) Degree Bias Comparison; (b)(c) r, α, β Sensitivity Analysis on Cora Dataset

than 2% across different parameter combinations. However, when β is particularly small (close to 0), a noticeable decline occurs. This implies that ignoring negative samples can cause the loss function to rely solely on positive samples, and can hinder effective contrastive learning. The performance increases as r decreases, which aligns with our intuition that more data labelled can provide more information that benefits learning. A lower r indicates a higher proportion of labelled data in the first pre-training step, enabling the model to learn more feature patterns. Still, our model shows competitive performance despite of the performance drop with higher r values. Despite a performance drop with higher r values, our model still shows competitive performance. Notably, when using SHARP (with GCN layers) with only half labelled data ($r = 0.5$), we still achieve an F1-score of 0.8504. This surpasses the performance of 0.834 which uses GCNs alone with the entire labelled dataset for training.

4.2.4 Visualisations

To further compare the structure of the models' learned representations, we apply t-SNE (Van der Maaten and Hinton, 2008) to map the high-dimensional embedding features to a low-dimensional space for visualization. Figure 7 shows the visualisations (GAT Layer, $r = 0.3$), with the full comparison in Appendix B. Each point represents the t-SNE processed latent space of the node embedding, with colors indicating different label categories. SHARP displays the clearest decision boundaries of the seven categories in Cora and six categories in CiteSeer. For inter-class performance, SHARP pushes nodes from different classes further apart than other methods. It aligns with the principle of contrastive learning by distancing negative samples and validates the effectiveness of our designed HAR loss. For intra-class performance, SHARP also pulls same-class nodes more tightly together than other methods. It reduces degree bias by strengthening the connections of low-degree nodes to their class. We conclude that our SHARP can capture the underlying structure of the data more effectively. The superior inter-class and intraclass performance further validates SHARP's effectiveness in degree bias mitigation.

5 Conclusions

The paper proposes a novel contrastive loss called HAR to mitigate degree bias in node classification. HAR offers two main advantages: (1) it assigns more positives to each node, providing low-degree nodes with additional information; and (2) it assigns weights to positives and negatives adaptive to their learning hardness, allowing more focus on low-degree nodes and more information about them to be learned.

Both theoretical analysis and experiments vali-

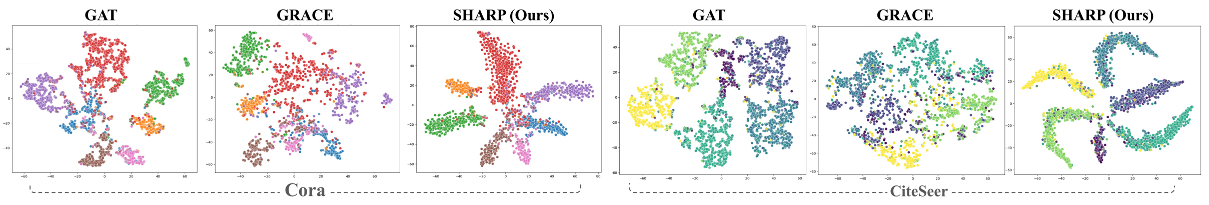

Figure 7: The t-SNE Visualizations of Embeddings on Cora and CiteSeer Dataset

date HAR's effectiveness. In the experiments, we design a two-step pipeline named SHARP to integrate and examine HAR's applicability in more diverse scenarios. Experiments on four datasets and comparisons with four baselines show that by focusing more on hard-to-learn nodes, the proposed SHARP can maintain good global performance while enhancing local performance for low-degree nodes, thereby reducing degree bias.

One limitation of the current work is that when the proportion of labelled data is particularly low (e.g., less than 30%), it can restrict the improvement of SHARP. One possible reason for this is that insufficient data can lead to a lack of feature information, which impacts graph representation learning. Future work could further explore using pre-trained models to add richer semantic information to low-degree nodes (Zhao et al., 2022; Yan et al., 2023), as well as extend this approach to more diverse scenarios such as heterogeneous graphs.

References

Mahmoud Assran, Nicolas Ballas, Lluis Castrejon, and Michael Rabbat. 2020. Supervision accelerates pre-training in contrastive semi-supervised learning of visual representations. *arXiv preprint arXiv:2006.10803*.

Michael M Bronstein, Joan Bruna, Taco Cohen, and Petar Veličković. 2021. Geometric deep learning: Grids, groups, graphs, geodesics, and gauges. *arXiv preprint arXiv:2104.13478*.

Ting Chen, Simon Kornblith, Mohammad Norouzi, and Geoffrey Hinton. 2020. A simple framework for contrastive learning of visual representations. In *International conference on machine learning*, pages 1597–1607. PMLR.

Ching-Yao Chuang, Joshua Robinson, Yen-Chen Lin, Antonio Torralba, and Stefanie Jegelka. 2020. Debiased contrastive learning. *Advances in neural information processing systems*, 33:8765–8775.

Fuli Feng, Weiran Huang, Xiangnan He, Xin Xin, Qifan Wang, and Tat-Seng Chua. 2021. Should graph convolution trust neighbors? a simple causal inference method. In *Proceedings of the 44th International ACM SIGIR Conference on Research and Development in Information Retrieval*, pages 1208–1218.

Matthias Fey and Jan E. Lenssen. 2019. Fast graph representation learning with PyTorch Geometric. In *ICLR Workshop on Representation Learning on Graphs and Manifolds*.

C Lee Giles, Kurt D Bollacker, and Steve Lawrence. 1998. Citeseer: An automatic citation indexing system. In *Proceedings of the third ACM conference on Digital libraries*, pages 89–98.

Will Hamilton, Zhitao Ying, and Jure Leskovec. 2017. Inductive representation learning on large graphs. *Advances in neural information processing systems*, 30.

Xiaotian Han, Kaixiong Zhou, Ting-Hsiang Wang, Jundong Li, Fei Wang, and Na Zou. 2024. Marginal nodes matter: Towards structure fairness in graphs. *ACM SIGKDD Explorations Newsletter*, 25(2):4–13.

Kaiming He, Haoqi Fan, Yuxin Wu, Saining Xie, and Ross Girshick. 2020. Momentum contrast for unsupervised visual representation learning. In *Proceedings of the IEEE/CVF conference on computer vision and pattern recognition*, pages 9729–9738.

Yannis Kalantidis, Mert Bulent Sariyildiz, Noe Pion, Philippe Weinzaepfel, and Diane Larlus. 2020. Hard negative mixing for contrastive learning. *Advances in neural information processing systems*, 33:21798–21809.

Jian Kang and Hanghang Tong. 2021. Fair graph mining. In *Proceedings of the 30th ACM International Conference on Information & Knowledge Management*, pages 4849–4852.

Prannay Khosla, Piotr Teterwak, Chen Wang, Aaron Sarna, Yonglong Tian, Phillip Isola, Aaron Maschinot, Ce Liu, and Dilip Krishnan. 2020. Supervised contrastive learning. *Advances in neural information processing systems*, 33:18661–18673.

Thomas N Kipf and Max Welling. 2016. Semi-supervised classification with graph convolutional networks. *arXiv preprint arXiv:1609.02907*.

Oyku Deniz Kose and Yanning Shen. 2022. Fair contrastive learning on graphs. *IEEE Transactions on Signal and Information Processing over Networks*, 8:475–488.

Junnan Li, Caiming Xiong, and Steven CH Hoi. 2021. Comatch: Semi-supervised learning with contrastive graph regularization. In *Proceedings of the IEEE/CVF international conference on computer vision*, pages 9475–9484.

Langzhang Liang, Zenglin Xu, Zixing Song, Irwin King, Yuan Qi, and Jieping Ye. 2023. Tackling long-tailed distribution issue in graph neural networks via normalization. *IEEE Transactions on Knowledge and Data Engineering*.

Hongyi Ling, Zhimeng Jiang, Youzhi Luo, Shuiwang Ji, and Na Zou. 2023. Learning fair graph representations via automated data augmentations. In *International Conference on Learning Representations (ICLR)*.

Zemin Liu, Trung-Kien Nguyen, and Yuan Fang. 2021. Tail-gnn: Tail-node graph neural networks. In *Proceedings of the 27th ACM SIGKDD Conference on Knowledge Discovery & Data Mining*, pages 1109–1119.

Zemin Liu, Trung-Kien Nguyen, and Yuan Fang. 2023. On generalized degree fairness in graph neural networks. In *Proceedings of the AAAI Conference on Artificial Intelligence*, volume 37, pages 4525–4533.

Andrew Kachites McCallum, Kamal Nigam, Jason Rennie, and Kristie Seymore. 2000. Automating the construction of internet portals with machine learning. *Information Retrieval*, 3:127–163.

Péter Mernyei and Cătălina Cangea. 2020. Wiki-cs: A wikipedia-based benchmark for graph neural networks. *arXiv preprint arXiv:2007.02901*.

Aaron van den Oord, Yazhe Li, and Oriol Vinyals. 2018. Representation learning with contrastive predictive coding. *arXiv preprint arXiv:1807.03748*.

Joshua Robinson, Ching-Yao Chuang, Suvrit Sra, and Stefanie Jegelka. 2021. Contrastive learning with hard negative samples. *International Conference on Learning Representations (ICLR)*.

Prithviraj Sen, Galileo Namata, Mustafa Bilgic, Lise Getoor, Brian Galligher, and Tina Eliassi-Rad. 2008. Collective classification in network data. *AI magazine*, 29(3):93–93.

Nitish Srivastava, Geoffrey Hinton, Alex Krizhevsky, Ilya Sutskever, and Ruslan Salakhutdinov. 2014. Dropout: a simple way to prevent neural networks from overfitting. *The journal of machine learning research*, 15(1):1929–1958.

Arjun Subramonian, Jian Kang, and Yizhou Sun. 2024. Theoretical and empirical insights into the origins of degree bias in graph neural networks. *arXiv preprint arXiv:2404.03139*.

Xianfeng Tang, Huaxiu Yao, Yiwei Sun, Yiqi Wang, Jiliang Tang, Charu Aggarwal, Prasenjit Mitra, and Suhang Wang. 2020. Investigating and mitigating degree-related biases in graph convoltuional networks. In *Proceedings of the 29th ACM International Conference on Information & Knowledge Management*, pages 1435–1444.

Laurens Van der Maaten and Geoffrey Hinton. 2008. Visualizing data using t-sne. *Journal of machine learning research*, 9(11).

Petar Veličković, Guillem Cucurull, Arantxa Casanova, Adriana Romero, Pietro Liò, and Yoshua Bengio. 2017. Graph attention networks. *6th International Conference on Learning Representations*.

Ruijia Wang, Xiao Wang, Chuan Shi, and Le Song. 2022. Uncovering the structural fairness in graph contrastive learning. *Advances in neural information processing systems*, 35:32465–32473.

Teng Xiao, Zhengyu Chen, Donglin Wang, and Suhang Wang. 2021. Learning how to propagate messages in graph neural networks. In *Proceedings of the 27th ACM SIGKDD Conference on Knowledge Discovery & Data Mining*, pages 1894–1903.

Hao Yan, Chaozhuo Li, Ruosong Long, Chao Yan, Jianan Zhao, Wenwen Zhuang, Jun Yin, Peiyan Zhang, Weihao Han, Hao Sun, et al. 2023. A comprehensive study on text-attributed graphs: Benchmarking and rethinking. *Advances in Neural Information Processing Systems*, 36:17238–17264.

Sukwon Yun, Kibum Kim, Kanghoon Yoon, and Chanyoung Park. 2022. Lte4g: Long-tail experts for graph neural networks. In *Proceedings of the 31st ACM International Conference on Information & Knowledge Management*, pages 2434–2443.

Shengzhong Zhang, Wenjie Yang, Yimin Zhang, Hongwei Zhang, Divin Yan, and Zengfeng Huang. 2023. Understanding community bias amplification in graph representation learning. *arXiv preprint arXiv:2312.04883*.

Mingxia Zhao and Adele Lu Jia. 2024. Dahgn: Degree-aware heterogeneous graph neural network. *Knowledge-Based Systems*, 285:111355.

Shuai Zhao, Tianyu Zhang, Man Hu, Wen Chang, and Fucheng You. 2022. Ap-bert: enhanced pre-trained model through average pooling. *Applied Intelligence*, 52(14):15929–15937.

Yanqiao Zhu, Yichen Xu, Feng Yu, Qiang Liu, Shu Wu, and Liang Wang. 2020. Deep graph contrastive representation learning. In *ICML Workshop on Graph Representation Learning and Beyond*.

Yanqiao Zhu, Yichen Xu, Feng Yu, Qiang Liu, Shu Wu, and Liang Wang. 2021. Graph contrastive learning with adaptive augmentation. In *Proceedings of the web conference 2021*, pages 2069–2080.

A Detailed Related Work of Graph Representation Learning

This section provides a detailed discussion of related work. Graph representation learning embeds graph-structured data into a feature space. The learned graph representations are generally integrated with task-specific neural networks to perform downstream tasks at various levels: graph-level, link-level, or node-level. This paper focuses on node-level tasks, which aim to predict the label of each node in a graph. GNNs and GCL are two common ways of generating embeddings for node classification tasks.

Graph Neural Networks (GNNs) are proposed to extend neural networks to process graph-structured data which has nodes features and connections between nodes. The core idea of GNNs is message passing between nodes, updating feature values by considering connected nodes layer by layer. Graph layers (GLs) define how nodes send, receive, and update messages. Convolution-based (e.g., GCN (Kipf and Welling, 2016)), attention-based (e.g., GAT (Veličković et al., 2017)), and aggregation-based (e.g., GraphSAGE (Hamilton et al., 2017)) are three common types of graph layers (Bronstein et al., 2021).

GCN aggregates using constant-weighted averages of neighbor messages. The layer-wise propagation rule of the GCN is as follows, where $\tilde{A}$ refers to the adjacency matrix A plus self-loops, $\tilde{D}$ is the degree matrix of $\tilde{A}$, $W^{(l)}$ is the trainable weight matrix, and $H^{(l)}$ is the activation matrix at layer l. $H^{(0)}$ equals the feature matrix X at layer $l = 0$.

$$H^{(l+1)} = \sigma\left(\hat{A}H^{(l)}W^{(l)}\right), \text{where} \hat{A} = \tilde{D}^{-\frac{1}{2}}\tilde{A}\tilde{D}^{-\frac{1}{2}} \tag{12}$$

Based on the idea of GCN, Graph Attention Network (GAT) adds attention mechanisms to learn the importance of neighboring nodes when aggregating feature information. GraphSAGE samples a subset of neighbors to reduce computational complexity for nodes with massive degrees.

Graph Contrastive Learning (GCL) combines GNNs with Contrastive Learning (CL) which enhances the robustness of learned representations. CL is a learning scheme that focuses on pulling similar/positive samples closer while pushing dissimilar/negative samples away using a contrastive loss (Chen et al., 2020). There are different contrastive loss definitions to ensure positive samples are brought together while negative samples are distanced effectively in GCL. The classic SimCLR (Chen et al., 2020) extends the usage of InfoNCE (Oord et al., 2018) in contrastive learning, aiming to learn representations by maximizing agreement between differently augmented views of the same sample in the latent space. Supervised contrastive learning (SCL) (Khosla et al., 2020) uses label information to more accurately identify positive samples as those from the same class, while negative samples are those from different classes. (Assran et al., 2020; Li et al., 2021) share a similar idea in the semi-supervised setting. Instead of treating all samples as equally important, (Robinson et al., 2021) proposes to assign adaptive weights for negative samples when calculating contrastive loss. Specifically, they focus on hard negative samples, which have high similarity but actually belong to different classes. They prove that these samples are harder to learn from and are worth assigning higher weights.

Specifically, for a given graph $G_i \in G$, SimCLR treats differently augmented views of the same sample as the positive pair $\{\tilde{z_i}', \tilde{z_i}''\}$, the remaining $2 \times (N-1)$ augmented samples are treated as negatives, denoted as $G_{\text{neg}} = \{G \setminus G_i\}$. Equation (13) defines the SimCLR loss for the positive pair $\{i, j\}$, τ is a temperature parameter used to scale the sim$(\cdot,\cdot)$, and $\mathbb{I}_{[k\neq i]}$ is an indicator function used to exclude comparisons with itself.

$$\ell_{i,j} = -\log \frac{f_\tau(z_i, z_j)}{\sum_{k=1}^{2N} \mathbb{I}_{[k\neq i]} f_\tau(z_i, z_k)} \tag{13}$$

In node classification task, GRACE (Zhu et al., 2020) generates contrastive views by randomly masking both nodes and edges, and considers the inter-view and intra-view negative pairs when designing the contrastive loss. For each node $v_i \in V$, let the representations of the augmented views be denoted as z_i' and z_i''. The GRACE loss is then defined as Equation (14).

$$\ell(z_i', z_i'') = -\log \frac{f_\tau(z_i', z_i'')}{f_\tau(z_i', z_i'') + \sum\limits_{k=1}^{N} \mathbb{I}_{[k\neq i]} f_\tau(z_i', z_k') + \sum\limits_{k=1}^{N} \mathbb{I}_{[k\neq i]} f_\tau(z_i', z_k'')} \tag{14}$$

B Details of Experiments

Settings We fixed the weight decay to $1e-5$. The feature dropping rate p_f, and edge drop rate p_e, are in the range [0, 0.4], the reweighting factors α and β are in the range (0, 1]. The early stop K rounds is set to 20. More differentiated parameter settings across different datasets are shown in Table 5, where 'Neurons' represents the number of neurons in the hidden and project hidden layers.

Table 5: Parameters Settings on Different Datasets

Dataset	τ	Neurons	Epoch	Learning Rate	Activation
Cora	0.4	128	300	5e-4	relu
Citeseer	0.9	256	300	1e-3	prelu
Pubmed	0.7	256	350	1e-3	relu
Wiki-CS	0.4	256	350	1e-2	relu

The evaluation metrics used in the paper are defined as below.

$$\text{Precision} = \frac{TP}{TP+FP}, \text{Recall} = \frac{TP}{TP+FN}, \text{F1-score} = \frac{2 \cdot \text{Precision} \cdot \text{Recall}}{\text{Precision} + \text{Recall}} \tag{15}$$

Degree Level Results The tables below provide supplementary results for degree-level performance analysis on Cora and PubMed datasets. For the Cora dataset, SHARP displayed the most significant global performance improvement. At the degree-level analysis, it also improved predictions for low-degree nodes. For the PubMed dataset, SHARP showed least global performance improvements. However, at the degree-level analysis, SHARP still improved the prediction of low-degree node.

Table 6: Comparison of Degree-level Prediction F1-score Across Models on Cora Dataset (GCN as the foundation graph layer, $r = 0$, Δ indicates difference with GCN)

Degree	Size	GCN	GRACE	Δ	SCL	Δ	Debias	Δ	SHARP(Ours)	Δ
1	161	0.7143	0.7323	1.80%	0.7565	4.22%	0.7758	6.15%	0.8081	**9.38%**
2	226	0.8319	0.8208	-1.11%	0.8000	-3.19%	0.8128	-1.91%	0.8504	**1.85%**
3	223	0.8341	0.7987	-3.54%	0.783	-5.11%	0.7892	-4.49%	0.8744	**4.03%**
4	134	0.9030	0.8373	-6.57%	0.8299	-7.31%	0.8507	-5.23%	0.9194	**1.64%**
5	101	0.8713	0.8861	1.48%	0.8337	-3.76%	0.8673	-0.40%	0.9050	**3.37%**
6	52	0.8077	0.7385	-6.92%	0.7212	-8.65%	0.7615	-4.62%	0.7865	-2.12%
7	25	0.8000	0.8280	2.80%	0.7960	-0.40%	0.8240	2.40%	0.8720	**7.20%**

Table 7: Comparison of Degree-level Prediction F1-score Across Models on Cora Dataset (GCN as the foundation graph layer, $r = 0.3$, Δ indicates difference with GCN)

Degree	Size	GCN	GRACE	Δ	SCL	Δ	Debias	Δ	SHARP(Ours)	Δ
1	161	0.7081	0.7012	-0.69%	0.7665	5.84%	0.7466	3.85%	0.8174	**10.93%**
2	226	0.8009	0.7867	-1.42%	0.8049	0.40%	0.7872	-1.37%	0.8358	**3.49%**
3	223	0.8206	0.7623	-5.83%	0.783	-3.76%	0.7677	-5.29%	0.8538	**3.32%**
4	134	0.9104	0.8224	-8.80%	0.8582	-5.22%	0.8313	-7.91%	0.9112	**0.08%**
5	101	0.8416	0.8663	2.47%	0.8871	4.55%	0.8653	2.37%	0.9079	**6.63%**
6	52	0.7308	0.7365	0.57%	0.7423	1.15%	0.7173	-1.35%	0.7654	**3.46%**
7	25	0.8400	0.7760	-6.40%	0.8160	-2.40%	0.8000	-4.00%	0.9280	**8.80%**

Table 8: Comparison of Degree-level Prediction Performance on Cora Dataset (GAT as the graph layer, $r = 0$, Δ indicates difference with the baseline GAT)

Degree	Size	GAT	GRACE	Δ	SCL	Δ	Debias	Δ	SHARP(Ours)	Δ
1	161	0.7143	0.7137	-0.06%	0.7702	5.59%	0.7944	8.01%	0.8106	**9.63%**
2	226	0.8186	0.8181	-0.05%	0.815	-0.36%	0.8283	0.97%	0.869	**5.04%**
3	223	0.8475	0.8027	-4.48%	0.8045	-4.30%	0.8323	-1.52%	0.8857	**3.82%**
4	134	0.8955	0.8455	-5.00%	0.8478	-4.77%	0.8672	-2.83%	0.9269	**3.14%**
5	101	0.8713	0.8782	0.69%	0.8495	-2.18%	0.8693	-0.20%	0.9059	**3.46%**
6	52	0.8462	0.7558	-9.04%	0.7577	-8.85%	0.7731	-7.31%	0.7846	-6.16%
7	25	0.8800	0.8240	-5.60%	0.7680	-11.20%	0.7760	-10.40%	0.8800	**0.00%**

Table 9: Comparison of Degree-level Prediction F1-score Across Models on Cora Dataset (GAT as the foundation graph layer, $r = 0.3$, Δ indicates changes compared with GAT)

Degree	Size	GAT	GRACE	Δ	SCL	Δ	Debias	Δ	SHARP(Ours)	Δ
1	161	0.7081	0.7075	-0.06%	0.7689	6.08%	0.7882	8.01%	0.8273	**11.92%**
2	226	0.8097	0.7996	-1.01%	0.8066	-0.31%	0.8155	0.58%	0.8597	**5.00%**
3	223	0.8296	0.8148	-1.48%	0.8018	-2.78%	0.8036	-2.60%	0.8525	**2.29%**
4	134	0.9030	0.8336	-6.94%	0.8724	-3.06%	0.8604	-4.26%	0.9164	**1.34%**
5	101	0.9010	0.8762	-2.48%	0.8891	-1.19%	0.8772	-2.38%	0.8921	-0.89%
6	52	0.7692	0.7731	0.39%	0.7615	-0.77%	0.7865	1.73%	0.7904	**2.12%**
7	25	0.8800	0.8200	-6.00%	0.7760	-10.40%	0.8040	-7.60%	0.9240	**4.40%**

Table 10: Comparison of Degree-level Prediction F1-score Across Models on PubMed Dataset (GCN as the foundation graph layer, $r = 0$, Δ indicates difference with GCN)

Degree	Size	GCN	GRACE	Δ	SCL	Δ	Debias	Δ	SHARP(Ours)	Δ
1	483	0.8406	0.8077	-3.29%	0.8685	2.79%	0.8638	2.32%	0.8712	**3.06%**
2	153	0.8824	0.8497	-3.27%	0.9307	**4.83%**	0.9275	4.51%	0.9157	**3.33%**
3	79	0.9494	0.9203	-2.91%	0.9658	1.64%	0.9557	0.63%	0.9620	**1.26%**
4	40	0.9000	0.8650	-3.50%	0.9500	5.00%	0.9500	5.00%	0.9675	**6.75%**
5	35	0.9143	0.8686	-4.57%	0.9514	**3.71%**	0.9400	**2.57%**	0.9286	1.43%
6	28	0.9643	0.8893	-7.50%	0.8929	**-7.14%**	0.8929	**-7.14%**	0.8929	**-7.14%**
7	14	0.9286	0.9571	2.85%	0.9429	**1.43%**	0.9786	5.00%	0.9929	**6.43%**

Visualisation Results Figure 8 shows t-SNE visualization on all methods (SHARP and baselines). SHARP displays the clearest class boundaries across all datasets.

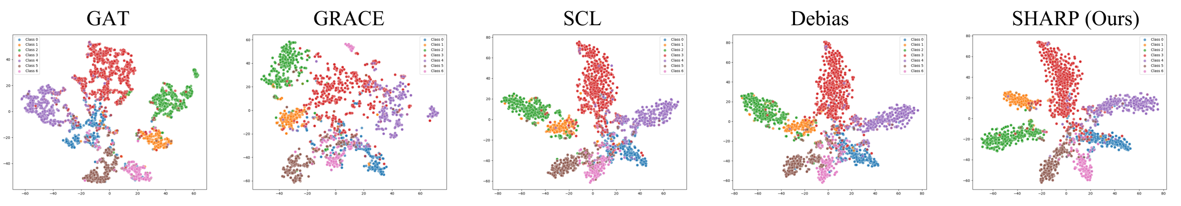

(a) Cora dataset

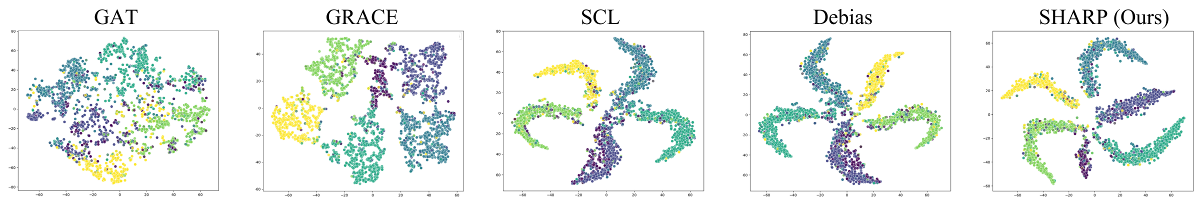

(b) Citeseer dataset

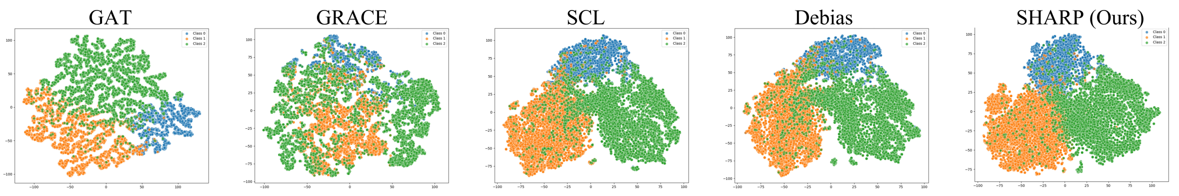

(c) PubMed dataset

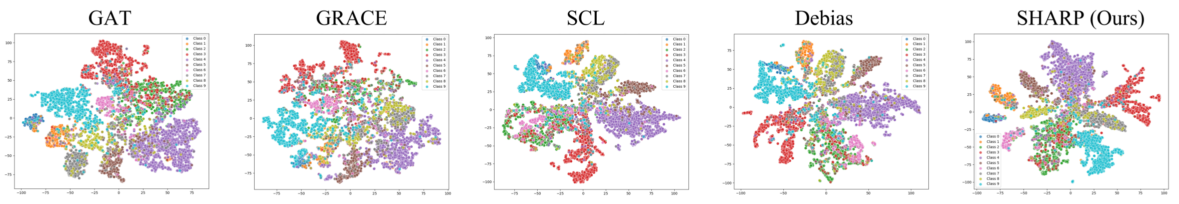

(d) Wiki-CS dataset

Figure 8: The t-SNE visualizations of embeddings on different models (GAT Layer, $r = 0.3$)

C Theoretical Analysis of Worst-case Scenario

This section presents an analysis based on the work of Robinson et al. (Robinson et al., 2021). In contrast to the approach described in (Robinson et al., 2021), which samples from an underlying distribution based on similarity in unsupervised learning, our method employs a sigmoid classifier $\sigma(z) : \mathcal{Z} \times \mathcal{C} \to [0, 1]$ on representation space $\mathcal{Z}$. This classifier is trained on labelled data to predict the unlabelled data, with marginal distribution $p(x)$. The positive and negative samples are associated with the distributions $x^+ \sim q^+$ and $x^- \sim q^-$, respectively, and are related to the embedding function. With slight abuse of notations, we refer to the embedding function as g. Specifically:

$$q^+_\alpha(x^+) \propto (e^{g(x)g(x^+)} + \alpha e^{-g(x)g(x^+)}) \cdot \sigma_{\text{sigmoid}}(g_p(x^+))$$
$$q^-_\beta(x^-) \propto e^{\beta g(x)g(x^-)} \cdot \sigma_{\text{sigmoid}}(g_p(x^-))$$

where $\alpha, \beta \in (0, 1]$, g_p denotes the embedding function learned under p. Increasing the scalar α results in reduced weights for positive samples (note that it is the normalised weights), while increasing β leads to higher weights for negative samples in the underlying distribution. Given the symmetric property of the HAR loss function (Equations (11) and (10)), the loss function can be expressed as the expectation of positive and negative samples from the transformation. We can reformulate the following loss function $\mathcal{L}$ to align with previous work (Chuang et al., 2020; Robinson et al., 2021):

$$\mathcal{L}(g, \alpha, \beta) = \mathbb{E}_{x\sim\mathcal{T}, x^+\sim p^+}\left[-\log \frac{\mathrm{I}_\alpha}{\mathrm{I}_\alpha + \mathrm{II}} \right], \tag{16}$$

where

$$\begin{aligned} \mathrm{I}_\alpha &= \mathbb{E}_{x^+ \in \{x'^+, x''^+\}}[e^{\bar{g}(x)\bar{g}(x^+)}] \\ &\quad + \alpha \mathbb{E}_{x^+ \notin \{x'^+, x''^+\}}[e^{-\bar{g}(x)\bar{g}(x^+)}], \\ \mathrm{II} &= \mathbb{E}_{x^- \sim q^-_\beta}[e^{\beta \bar{g}(x)\bar{g}(x^-)}]. \end{aligned}$$

Here, $\bar{g}(t) := g(t)/(\sqrt{\tau} \cdot \|g(t)\|)$ is the normalised embedding function, and we have the bounds $e^{-1/\tau} \le |e^{\bar{g}(u)\bar{g}(v)}| \le e^{1/\tau}$ for any $u, v \in \mathcal{X}$. $\{x'^+, x''^+\}$ refers to the set of the pairs under graph argumentation. The first part of I_α refers to the pairs of (two) data points after augmentation, while the second term is greater than 0. Taking $\alpha = 0$, the Equation (16) degenerates to the case described in (Robinson et al., 2021). Further, given fixed β and by monotonicity property of logarithm function, we observe that the upper bound of loss function is reached when $\alpha = 0$ (w.r.t. the "lower" classification performance), Therefore, we have the following proposition:

PROPOSITION C.1. *With a fixed β and when $\alpha = 0$, the worst-case performance of SHARP is bounded by the performance of an unsupervised method (Robinson et al., 2021). That is, the SHARP's worst-case performance is when SHARP degenerates to an unsupervised contrastive learning approach.*

Before analysing $\mathcal{L}(g, \beta) := \mathcal{L}(g, 0, \beta)$, one may note that the classifier is learned on a labelled dataset. Intuitively, the classifier can assign higher weights to negative samples than those obtained by directly sampling from the dataset. We have the following proposition:

PROPOSITION C.2. (SAMPLING RATIO) *The probability of a selected sample being a negative sample based on our method is at least equal to that of the probability of a randomly selected sample being a negative sample from the marginal distribution in (Robinson et al., 2021). That is, the sampling ratio $w(x^-)$ is at least greater than or equal to 1, and exists a constant,*

$$w(x^-) := \frac{\sigma_{sigmoid}(g_p(x^-))}{p(x^-)} \ge 1,$$

and

$$\mathbb{E}_{x^- \sim p^-}[w(x^-)] = \text{const.}$$

We have the following lemma on the worst-case objective function, building on the Proposition 3 in (Robinson et al., 2021).

LEMMA C.1. (WORST-CASE NEGATIVE SAMPLING) *When $\alpha = 0$, let $\bar{\mathcal{L}}(g) = \sup_\beta \mathcal{L}(g, \beta)$. For any $\tau > 0$, we have $\mathcal{L}(g, \beta) \to \bar{\mathcal{L}}(g)$ as $\beta \to \infty$.*

Proof. Similar to the proof in (Robinson et al., 2021), we consider the essential supremum,

$$M(x) = \sup \left\{ 0 < m \leq 1 : \begin{array}{l} \bar{g}(x)\bar{g}(x^-) \leq m, \\ \text{a.s. for } x^- \sim p^- \end{array} \right\},$$

with

$$\bar{\mathcal{L}}(g, \beta) = \mathbb{E}_{x \sim \mathcal{T}, x^+ \sim p^+} \left[-\log \frac{\mathrm{I}_{\alpha=0}}{\mathrm{I}_{\alpha=0} + \bar{Q} e^{M(x)}} \right],$$

where $\bar{Q}$ is a constant of upper bound of the ratio of negative samples to positive samples. Recall that in a balanced and binary classification, we may have $\bar{Q} = 1$. In cases of multi-class classification, $\bar{Q}$ is a constant chosen based on the ratio of the most imbalanced class for analysis. We have the difference of the two terms,

$$\begin{aligned} & \left| \bar{\mathcal{L}}(g) - \mathcal{L}(g, \beta) \right| \\ = & \, \mathbb{E}_{x \sim \mathcal{T}, x^+ \sim p^+} \left| \log \left(\bar{g}(x)\bar{g}(x^+) + \bar{Q} \mathbb{E}_{x^- \sim q_\beta^-} [\bar{g}(x)\bar{g}(x^-)] \right) \right. \\ & \left. - \log \left(\bar{g}(x)\bar{g}(x^+) + \bar{Q} e^{M(x)} \right) \right| \\ \leq & \, \frac{e^{1/\tau} \bar{Q}}{\bar{Q} + 1} \mathbb{E}_{x \sim \mathcal{T}} \mathbb{E}_{x^- \sim q_\beta^-} \left| e^{M(x)} - e^{\bar{g}(x)\bar{g}(x^-)} \right| \\ \leq & \, e^{2/\tau} \mathbb{E}_{x \sim \mathcal{T}} \mathbb{E}_{x^- \sim q_\beta^-} \left| M(x) - \bar{g}(x)\bar{g}(x^-) \right| \end{aligned}$$

Following prior work, the first inequality is due to Lipschitz of logarithm function and rearranging the terms. Note that the expectation does not contain terms with x^+. The second inequality is due to $|e^{\bar{g}(x)\bar{g}(x^-)}| \leq e^{1/\tau}$. Now we analyse the expectation of $|M(x) - \bar{g}(x)\bar{g}(x^-)|$. Given a fixed sample x, and a set of "good" events $\mathcal{G}_\epsilon = \{x^- : \bar{g}(x)\bar{g}(x^-) \geq M(x) - \epsilon\}$, and its complement set $\mathcal{G}_\epsilon^c$, for a fixed t and $\epsilon > 0$,

$$\begin{aligned} & \mathbb{E}_{x^- \sim q_\beta^-} \left| M(x) - \bar{g}(x)\bar{g}(x^-) \right| \\ = & \, \mathbb{P}_{x^- \sim q_\beta^-}(\mathcal{G}_\epsilon) \mathbb{E}_{x^- \sim q_\beta^-} \left[\left| M(x) - \bar{g}(x)\bar{g}(x^-) \right| | \mathcal{G}_\epsilon \right] \\ & + \mathbb{P}_{x^- \sim q_\beta^-}(\mathcal{G}_\epsilon^c) \mathbb{E}_{x^- \sim q_\beta^-} \left[\left| M(x) - \bar{g}(x)\bar{g}(x^-) \right| | \mathcal{G}_\epsilon^c \right] \\ \leq & \, \epsilon + 2 \mathbb{P}_{x^- \sim q_\beta^-}(\mathcal{G}_\epsilon^c) \end{aligned}$$

Further, with the Proposition C.2,

$$\begin{aligned} & \mathbb{P}_{x^- \sim q_\beta^-}(\mathcal{G}_\epsilon^c) \\ = & \int_{\mathcal{X}} \mathbb{I}_{(\bar{g}(x)\bar{g}(x^-) < M(x) - \epsilon)} \frac{e^{\beta g(x) g(x^-)} \cdot p(x^-)}{Z_\beta} \cdot w(x^-) \mathrm{d}x^- \\ \leq & \, \frac{e^{\beta(M(x) - \epsilon)}}{Z_\beta} \mathbb{E}_{x^- \sim p^-}[w(x^-)] \\ \leq & \, \frac{e^{\beta(M(x) - \epsilon)}}{Z_\beta} \cdot \text{const} \end{aligned}$$

where

$$\begin{aligned} Z_\beta &= \int_{\mathcal{X}} e^{\beta g(x) g(x^-)} \cdot \sigma_{\text{sigmoid}}(g_p(x^-)) \mathrm{d}x^- \\ &= \int_{\mathcal{X}} e^{\beta g(x) g(x^-)} \cdot p(x^-) \cdot \frac{\sigma_{\text{sigmoid}}(g_p(x^-))}{p(x^-)} \mathrm{d}x^- \\ &\geq e^{\beta(M-\epsilon/2)} \mathbb{P}_{x^- \sim p^-}(g(x)g(x^-) > M - \epsilon/2) \end{aligned}$$

With $\rho_\epsilon := \mathbb{P}_{x^- \sim p^-}\left((\bar{g}(x^-)\bar{g}(x^-) \leq M(x) - \epsilon/2)\right) > 0$, similarly, with $\beta \to \infty$ we have

$$\mathbb{P}_{x^- \sim q_\beta^-}(\mathcal{G}_\epsilon^c) \leq \frac{e^{\beta(M(x)-\epsilon)}}{e^{\beta(M(x)-\epsilon/2)}} \cdot \rho_\epsilon^{-1} = e^{-\beta\epsilon/2}\rho_\epsilon^{-1} \to 0$$

We have the term $\left|\bar{\mathcal{L}}(g) - \mathcal{L}(g, \beta)\right| \to 0$ with sufficient small ϵ. □

This proposition also suggests that the theorems provided in (Robinson et al., 2021) hold. We provide a brief interpretation of the theorems for reference, the Lemma C.2 and C.3.

LEMMA C.2. (THEOREM 4 IN (ROBINSON ET AL., 2021), INFORMAL) *The downstream classification task can be viewed as a packing problem. The solution of minimising the $\bar{\mathcal{L}}(g)$ are a maximum margin clustering in packing problem.*

LEMMA C.3. (THEOREM 5 IN (ROBINSON ET AL., 2021), INFORMAL) *Under Lemma C.2, there exists a solution to the packing problem achieving bounded misclassification risk for the downstream classifier.*

For the proof of the lemmas, we refer readers to see the Appendix A2 in (Robinson et al., 2021). Overall, it suggests that regarding the selection of hyper-parameters, if the classifier achieves adequate performance than random sampling, the performance is better than purely unsupervised case. Based on all the above analysis, we have the following corollary:

COROLLARY C.1. *The misclassification risk of SHARP is bounded, and the objective function of SHARP is not higher than that of the unsupervised objective function in (Robinson et al., 2021).*